ELSEVIER

Bifurcation of limit cycles in a quintic Hamiltonian system under a sixth-order perturbation

S. Wang, P. Yu *

Department of Applied Mathematics, The University of Western Ontario, London, Ont., Canada N6A 5B7

Accepted 29 March 2005

Communicated by Prof. He Ji Huan

Abstract

This paper intends to explore the bifurcation of limit cycles for planar polynomial systems with even number of degrees. To obtain the maximum number of limit cycles, a sixth-order polynomial perturbation is added to a quintic Hamiltonian system, and both local and global bifurcations are considered. By employing the detection function method for global bifurcations of limit cycles and the normal form theory for local degenerate Hopf bifurcations, 31 and 35 limit cycles and their configurations are obtained for different sets of controlled parameters. It is shown that: $H(6) \geqslant 35 = 6^2 - 1$, where $H(6)$ is the Hilbert number for sixth-degree polynomial systems.
© 2005 Elsevier Ltd. All rights reserved.

1. Introduction

The second part of Hilbert's 16th problem is concerned with the number of limit cycles of planar polynomial differential equations. It remains unsolved even for quadratic polynomial systems. But this problem has inspired significant progress in geometric theory, bifurcation theory, normal forms and algebraic geometry [1].

Due to persistence of the problem, it makes sense to consider simplified versions in advance [2]. In 1977, Arnold [3] posed a ''weakened'' Hilbert 16th problem which seeks bounds on the number of limit cycles which occur in perturbed Hamiltonian systems [4]. A number of results have been published regarding the lower bounds of the number of limit cycles in perturbed Hamiltonian systems. Some of them focus on local bifurcations at non-hyperbolic equilibrium points [5–7], while others deal with global bifurcations from homoclinic (or heteroclinic) loops or periodic orbits based on the Melnikov method [8,10,9,11–15].

It has been noted that most articles related to the weakened Hilbert 16th problem consider odd degree of polynomial Hamiltonian systems, taking advantage of the symmetric distribution of algebraic curves in odd degree planar polynomial systems. With symmetric odd degree perturbations, the systems are able to generate more limit cycles at a given degree. On other hand, even degree systems are equally important as odd degree systems, but very few results have been

---

* Corresponding author. Fax: +1 519 661 3523.
  E-mail address: pyu@pyu1.apmaths.uwo.ca (P. Yu).

achieved. This is the major motivation of this paper to study bifurcation of limit cycles in even degree polynomial systems.

The lowest even degree polynomial systems are quadratic systems, which have been intensively studied (e.g. see [9,10,14–17]) with the best result of $H(2) \geqslant 4$. Recently, $H(4) \geqslant 15$ has been reported by Zhang et al. [11] based on a cubic system with quartic perturbations. Thus we study bifurcations of limit cycles in sixth-degree polynomial systems. To approach the maximal number of limit cycles, both local and global bifurcations are considered in choosing control parameters. The detection function method [18] is applied to compute global limit cycles, while an early developed normal form computation technique [19] is employed in calculating local focus values to examine small limit cycles.

Bifurcation of limit cycles and symmetry are closely connected [19], and symmetric Hamiltonian systems exhibit great advantage in the study of global limit cycles, by using the detection function method. Desire not to completely lose this advantage in our investigation of even degree polynomial systems, we will add a sixth-degree polynomial perturbation to a fifth-degree Z_2 symmetric polynomial Hamiltonian system to examine the highest lower bound of the number of limit cycles for the sixth-degree polynomial system. The sixth-degree perturbation is expected to break the symmetry. However, on the other hand, when all the possible terms are included, it gains more flexibility in setting up control equations with more parameters comparing with fifth-degree symmetric perturbations [21,22]. Such flexibility also extends to combining more local Hopf bifurcation conditions into parameter control.

We begin with a Z_2-equivariant Hamiltonian system of degree 5, given by

$$
\begin{aligned}
\frac{\mathrm{d}x}{\mathrm{d}t} &= y\left(1 - \frac{1}{2}y^2\right)\left(1 - \frac{1}{8}y^2\right), \\
\frac{\mathrm{d}y}{\mathrm{d}t} &= -x(1 - 2x^2)\left(1 - \frac{1}{2}x^2\right).
\end{aligned}
\tag{1}
$$

This system was first studied by Chen et al. [21], who claimed that 29 limit cycles were obtained under the following quintic perturbation:

$$
\begin{aligned}
\frac{\mathrm{d}x}{\mathrm{d}t} &= y\left(1 - \frac{1}{2}y^2\right)\left(1 - \frac{1}{8}y^2\right), \\
\frac{\mathrm{d}y}{\mathrm{d}t} &= -x(1 - 2x^2)\left(1 - \frac{1}{2}x^2\right) + \epsilon y(\delta + \mu x^2 + r y^2 + k x^4 + n x^2 y^2 + y^4).
\end{aligned}
\tag{2}
$$

However, this result was later shown to be incorrect by Li et al. [22], who obtained maximal 23 limit cycles for the same system with the same perturbation.

In this paper, we investigate system (1) by adding more general sixth-degree polynomial perturbations, leading to a new system:

$$
\begin{aligned}
\frac{\mathrm{d}x}{\mathrm{d}t} &= y\left(1 - \frac{1}{2}y^2\right)\left(1 - \frac{1}{8}y^2\right) + \epsilon x\left(\sum_{1 \leqslant i+j \leqslant 5} a_{ij} x^i y^j - \lambda\right), \\
\frac{\mathrm{d}y}{\mathrm{d}t} &= -x(1 - 2x^2)\left(1 - \frac{1}{2}x^2\right) + \epsilon y\left(\sum_{1 \leqslant i+j \leqslant 5} b_{ij} x^i y^j - \lambda\right),
\end{aligned}
\tag{3}
$$

where $0 < \epsilon \ll 1$, a_{ij}'s and b_{ij}'s are parameters, and λ is a detection function [18] for detecting the number and locations of global limit cycles.

The rest of the paper is organized as follows. In Section 2, we will briefly describe the behavior of the unperturbed fifth-degree Hamiltonian system (1), followed by presenting a procedure of calculating bifurcation parameter values for the perturbed sixth-degree system using the detection function method. In Section 3, we will outline the normal form computation technique which will be used to calculate the focus values of local degenerate Hopf bifurcations. Section 4 is devoted to design parameter control by combining both global and local limit cycle computations and show two configurations of limit cycles for the sixth-degree polynomial system (3). The maximal number of limit cycles we obtain from this system is 35. Finally, conclusion is drawn in Section 5.

2. Computation of global bifurcations of limit cycles

We start from analyzing the global behavior of the unperturbed Hamiltonian system (1). The system has 25 critical points which locate symmetrically with respect to the *x*-axis and *y*-axis. Fig. 1 shows the phase portrait of the system
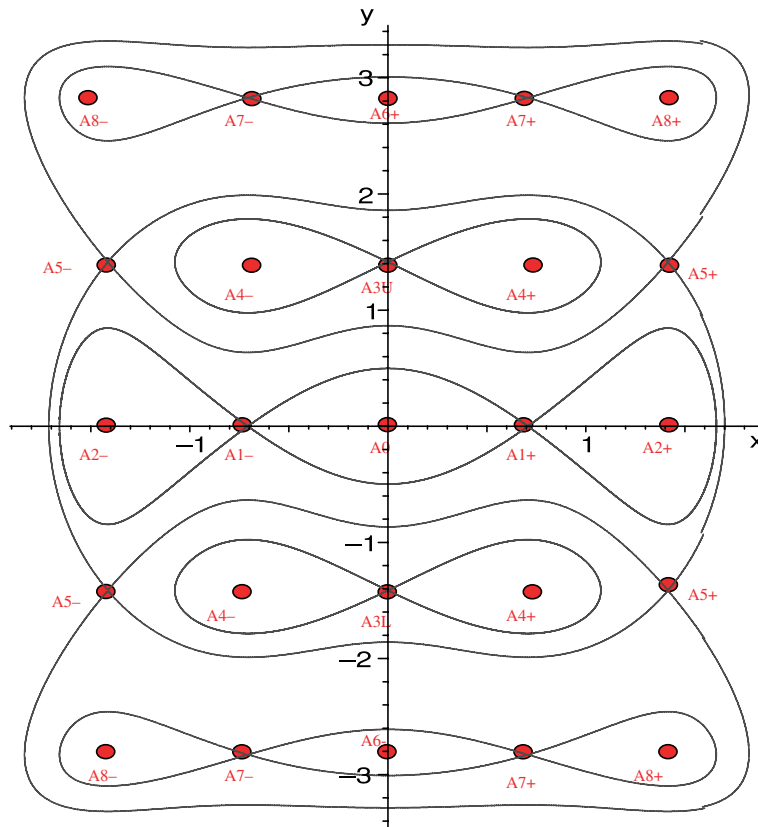
Fig. 1. Phase portrait and critical points of system (1).

and the locations of the 25 critical points, whose coordinates and types are listed in Table 1, where the 25 critical points are labelled as nine distinct groups as A_0, A_1, A_2, A_3, A_4, A_5, A_6, A_7, A_8 and A_9 according to their symmetric locations.

System (1) has the following Hamiltonian:

$$H(x,y) = \frac{1}{2}x^2 + \frac{1}{2}y^2 - \frac{5}{8}x^4 - \frac{5}{32}y^4 + \frac{1}{6}x^6 + \frac{1}{96}y^6, \tag{4}$$

Table 1
25 Critical points, U—upper half plane, L—lower half plane

No.	Notation	Coordinates	Type
0	A_0	$(0,0)$	Focus
1	$A_{1\pm}$	$(\pm\frac{1}{\sqrt{2}}, 0)$	Saddle
2	$A_{2\pm}$	$(\pm\sqrt{2}, 0)$	Focus
3	A_3^{UL}	$(0, \pm\sqrt{2})$	Saddle
4	$A_{4\pm}^{U}$	$(\pm\frac{1}{\sqrt{2}}, \sqrt{2})$	Focus
	$A_{4\pm}^{L}$	$(\pm\frac{1}{\sqrt{2}}, -\sqrt{2})$	
5	$A_{5\pm}^{U}$	$(\pm\sqrt{2}, \sqrt{2})$	Saddle
	$A_{5\pm}^{L}$	$(\pm\sqrt{2}, -\sqrt{2})$	
6	A_6^{UL}	$(0, \pm2\sqrt{2})$	Focus
7	$A_{7\pm}^{U}$	$(\pm\frac{1}{\sqrt{2}}, 2\sqrt{2})$	Saddle
	$A_{7\pm}^{L}$	$(\pm\frac{1}{\sqrt{2}}, -2\sqrt{2})$	
8	$A_{8\pm}^{U}$	$(\pm\sqrt{2}, 2\sqrt{2})$	Focus
	$A_{8\pm}^{L}$	$(\pm\sqrt{2}, -2\sqrt{2})$	

which is a symmetric sixth-degree polynomial function with respect to both the x-axis and the y-axis. Therefore, there are a total of 9 distinct Hamiltonian levels from the 9 groups of the 25 critical points, given as follows:

$$h_0 = H(A_0) = H(0,0) = 0,$$
$$h_1 = H(A_1) = H\left(\pm\frac{1}{\sqrt{2}}, 0\right) = \frac{11}{96} \approx 0.1145833333,$$
$$h_2 = H(A_2) = H(\pm\sqrt{2}, 0) = -\frac{11}{96} \approx -0.166666667,$$
$$h_3 = H(A_3) = H(0, \pm\sqrt{2}) = \frac{11}{24} \approx 0.4583333333,$$
$$h_4 = H(A_4) = H\left(\pm\sqrt{2}, \pm\frac{1}{\sqrt{2}}\right) = -\frac{55}{96} \approx 0.5729166667,$$
$$h_5 = H(A_5) = H(\pm\sqrt{2}, \pm\sqrt{2}) = \frac{7}{24} \approx 0.2916666667,$$
$$h_6 = H(A_6) = H\left(0, \pm2\sqrt{2}\right) = -\frac{2}{3} \approx -0.666666667,$$
$$h_7 = H(A_7) = H\left(\pm\frac{1}{\sqrt{2}}, \pm\sqrt{2}\right) = -\frac{53}{96} \approx -0.55203333,$$
$$h_8 = H(A_8) = H(\pm\sqrt{2}, \pm2\sqrt{2}) = -\frac{5}{6} \approx -0.833333333.$$

Since each critical point associates with one family of closed orbits, there are, in total, 25 closed orbits for the unperturbed Hamiltonian system. Fig. 2 shows the transition of algebraic curves with the increase of the level value.

Now, we add a sixth-degree polynomial perturbation to system (1). By taking the form of perturbation used in the detection function method [21], we apply a more general perturbation to obtain:

$$\frac{dx}{dt} = y\left(1 - \frac{1}{2}y^2\right)\left(1 - \frac{1}{8}y^2\right) + \epsilon x\left(\sum_{1 \leqslant i+j \leqslant 5} a_{ij}x^iy^j - \lambda\right),$$
$$\frac{dy}{dt} = -x(1 - 2x^2)\left(1 - \frac{1}{2}x^2\right) + \epsilon y\left(\sum_{1 \leqslant i+j \leqslant 5} b_{ij}x^iy^j - \lambda\right),$$
(5)

where $0 < \epsilon \ll 1$, $a_{i,j}$'s and $b_{i,j}$'s are parameters and λ is called detection function [20] which will be defined later to examine the numbers of global limit cycles for system (5). Consequently, the so-called Poincare-Melnikov Abelian integral [23] associated with system (5) can be written as

$$I(h) = \int_{\Gamma_h} x\left(\sum a_{ij}x^iy^j - \lambda\right)dy - y\left(\sum b_{ij}x^iy^j - \lambda\right)dx = \iint_{D_h}\left(\frac{\partial\left(\sum a_{ij}x^iy^j - \lambda\right)}{\partial x} + \frac{\partial\left(\sum b_{ij}x^iy^j - \lambda\right)}{\partial y}\right)dx\,dy$$
$$= \iint_{D_h}\left\{\sum[(1+i)a_{ij} + (1+j)b_{ij}]x^iy^j - 2\lambda\right\}dx\,dy,$$
(6)

where h is Hamiltonian level, Γ_h is a family of closed orbits corresponding to h, and D_h is the area inside Γ_h. According to the Poincare-Pontrjagin–Andronov theorem [20], the number of isolated zeros of the Abelian integral $I(h)$ is an upper bound of the number of limit cycles which bifurcate from this family of closed orbits. To study the number of limit cycles for the system, we set the Abelian integral $I(h) = 0$. The detection function can then be defined as

$$\lambda = \lambda(h) = \frac{\iint_{D_h} S(x,y)dx\,dy}{\iint_{D_h} dx\,dy} = \sum_{1 \leqslant i+j \leqslant 5} s_{ij}J_{ij}(h),$$
(7)

where

$$S(x,y) = \sum_{1 \leqslant i+j \leqslant 5} s_{ij}x^iy^j,$$
$$s_{ij} = \frac{1}{2}\left[(1+i)a_{ij} + (1+j)\right]b_{ij},$$
$$J_{ij}(h) = \frac{\psi_{ij}(h)}{\phi(h)},$$
(8)
$$\psi_{ij}(h) = \iint_{D_h} x^iy^j dx\,dy,$$
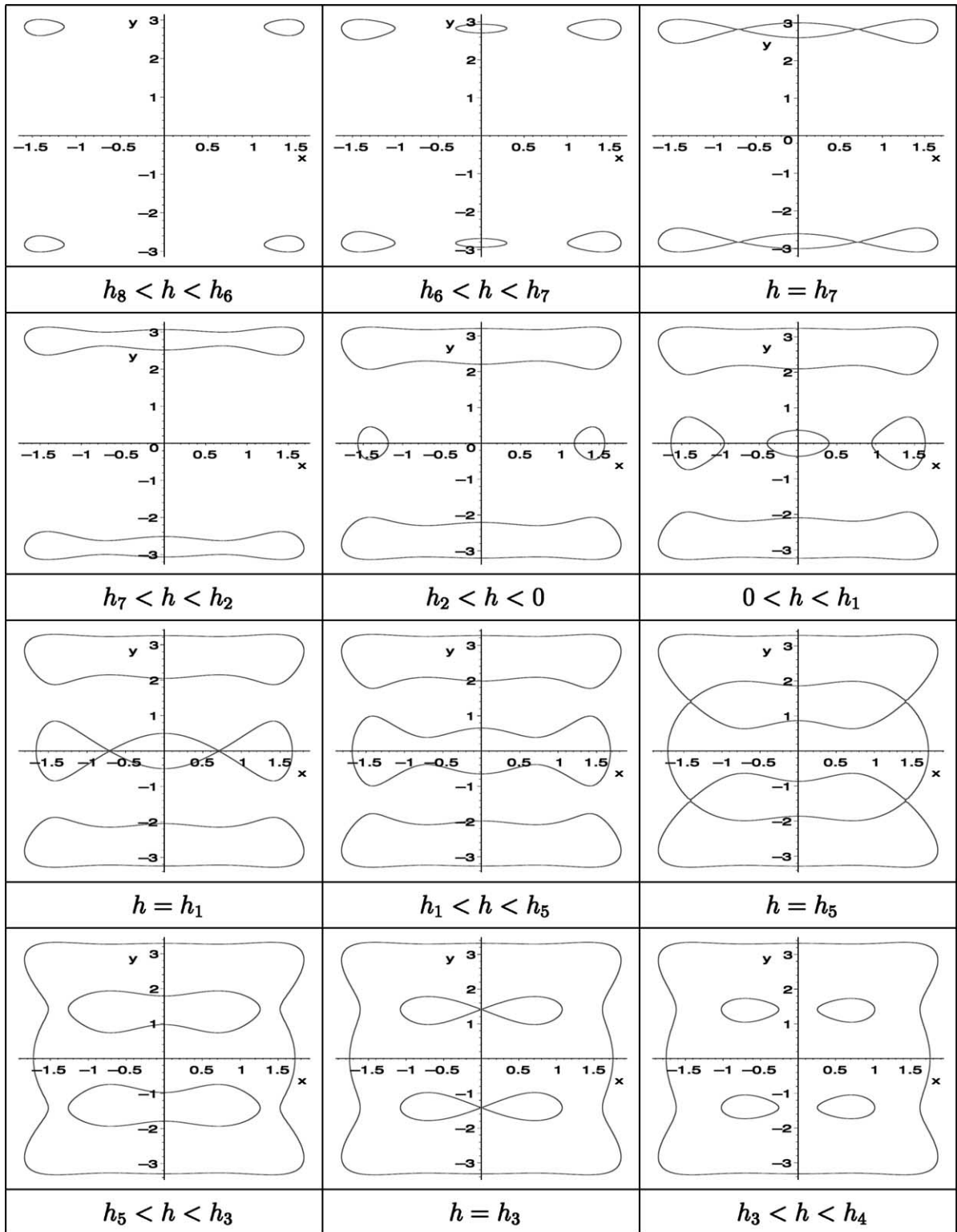$$\phi(h) = \iint_{D_h} dx\,dy.$$

Fig. 2. Flow chart of algebraic curves of system (1).

Table 2
First- and second-order focus values of Hopf bifurcations

Focus	v	Focus values
A_0	v_0	$\epsilon\lambda$
	v_1	$\epsilon\left(\dfrac{1}{4}s_{20} + \dfrac{1}{4}s_{02}\right) + O(\epsilon^2)$
A_{2-}	v_0	$\epsilon(4s_{20} + 8s_{40} - 2\sqrt{2}s_{10} - 4\sqrt{2}s_{30} - 8\sqrt{2}s_{50} - 2\lambda)$
	v_1	$\epsilon\left(\dfrac{19}{24}\sqrt{3}s_{30} + \dfrac{65}{36}\sqrt{3}s_{50} - \dfrac{1}{2}\sqrt{3}s_{12} + \dfrac{25}{144}\sqrt{3}s_{10} - \sqrt{3}s_{32} - \dfrac{1}{2}\sqrt{6}s_{22} - \dfrac{1}{4}\sqrt{6}s_{02} + \dfrac{11}{36}\sqrt{6}s_{20} + \dfrac{8}{9}\sqrt{6}s_{40}\right) + O(\epsilon^2)$
A_{2+}	v_0	$\epsilon(4s_{20} + 8s_{40} + 2\sqrt{2}s_{10} + 4\sqrt{2}s_{30} + 8\sqrt{2}s_{50} - 2\lambda)$
	v_1	$\epsilon\left(-\dfrac{19}{24}\sqrt{3}s_{30} - \dfrac{65}{36}\sqrt{3}s_{50} + \dfrac{1}{2}\sqrt{3}s_{12} - \dfrac{25}{144}\sqrt{3}s_{10} + \sqrt{3}s_{32} - \dfrac{1}{2}\sqrt{6}s_{22} - \dfrac{1}{4}\sqrt{6}s_{02} + \dfrac{11}{36}\sqrt{6}s_{20} + \dfrac{8}{9}\sqrt{6}s_{40}\right) + O(\epsilon^2)$
A_{4-}^U	v_0	$\epsilon\left(s_{20} + 4s_{02} + \dfrac{1}{2}s_{40} + 8s_{04} + 2s_{22} - \sqrt{2}s_{10} - \dfrac{1}{2}\sqrt{2}s_{30} - \dfrac{1}{4}\sqrt{2}s_{50} - 2\sqrt{2}s_{12} - 4\sqrt{2}s_{14} - \sqrt{2}s_{32} - 2\lambda\right)$
	v_1	$\epsilon\left(\dfrac{5}{36}\sqrt{2}s_{10} - \dfrac{1}{24}\sqrt{2}s_{30} + \dfrac{1}{3}\sqrt{2}s_{12} - \dfrac{1}{9}s_{02} + \dfrac{2}{9}s_{40} - \dfrac{5}{18}s_{22} + \dfrac{8}{9}s_{04} - \dfrac{1}{9}s_{20} - \dfrac{1}{18}\sqrt{2}s_{32} + \dfrac{1}{9}\sqrt{2}s_{14} - \dfrac{35}{144}\sqrt{2}s_{50}\right) + O(\epsilon^2)$
A_{4+}^U	v_0	$\epsilon\left(s_{20} + 4s_{02} + \dfrac{1}{2}s_{40} + 8s_{04} + 2s_{22} + \sqrt{2}s_{10} + \dfrac{1}{2}\sqrt{2}s_{30} + \dfrac{1}{4}\sqrt{2}s_{50} + 2\sqrt{2}s_{12} + 4\sqrt{2}s_{14} + \sqrt{2}s_{32} - 2\lambda\right)$
	v_1	$\epsilon\left(-\dfrac{5}{36}\sqrt{2}s_{10} + \dfrac{1}{24}\sqrt{2}s_{30} - \dfrac{1}{3}\sqrt{2}s_{12} - \dfrac{1}{9}s_{02} + \dfrac{2}{9}s_{40} - \dfrac{5}{18}s_{22} + \dfrac{8}{9}s_{04} - \dfrac{1}{9}s_{20} + \dfrac{1}{18}\sqrt{2}s_{32} - \dfrac{1}{9}\sqrt{2}s_{14} + \dfrac{35}{144}\sqrt{2}s_{50}\right) + O(\epsilon^2)$
A_6^U	v_0	$\epsilon(128s_{04} + 16s_{02} - 2\lambda)$
	v_1	$\epsilon\left(-\dfrac{32}{9}\sqrt{6}s_{04} + 2\sqrt{6}s_{22} - \dfrac{11}{36}\sqrt{6}s_{02} + \dfrac{1}{4}\sqrt{6}s_{20}\right) + O(\epsilon^2)$
A_{8-}^U	v_0	$\epsilon(4s_{20} + 16s_{02} + 8s_{40} + 128s_{04} + 32s_{22} - 2\sqrt{2}s_{10} - 4\sqrt{2}s_{30} - 8\sqrt{2}s_{50} - 16\sqrt{2}s_{12} - 128\sqrt{2}s_{14} - 32\sqrt{2}s_{32} - 2\lambda)$
	v_1	$\epsilon\left(\dfrac{25}{288}\sqrt{2}s_{10} + \dfrac{19}{48}\sqrt{2}s_{30} + \sqrt{2}s_{12} - \dfrac{11}{36}s_{02} - \dfrac{8}{9}s_{40} - \dfrac{55}{18}s_{22} - \dfrac{32}{9}s_{04} - \dfrac{11}{36}s_{20} + \dfrac{34}{9}\sqrt{2}s_{32} + \dfrac{82}{9}\sqrt{2}s_{14} + \dfrac{65}{72}\sqrt{2}s_{50}\right) + O(\epsilon^2)$
A_{8+}^U	v_0	$\epsilon(4s_{20} + 16s_{02} + 8s_{40} + 128s_{04} + 32s_{22} + 2\sqrt{2}s_{10} + 4\sqrt{2}s_{30} + 8\sqrt{2}s_{50} + 16\sqrt{2}s_{12} + 128\sqrt{2}s_{14} + 32\sqrt{2}s_{32} - 2\lambda)$
	v_1	$\epsilon\left(-\dfrac{25}{288}\sqrt{2}s_{10} - \dfrac{19}{48}\sqrt{2}s_{30} - \sqrt{2}s_{12} - \dfrac{11}{36}s_{02} - \dfrac{8}{9}s_{40} - \dfrac{55}{18}s_{22} - \dfrac{32}{9}s_{04} - \dfrac{11}{36}s_{20} - \dfrac{34}{9}\sqrt{2}s_{32} - \dfrac{82}{9}\sqrt{2}s_{14} - \dfrac{65}{72}\sqrt{2}s_{50}\right) + O(\epsilon^2)$

Clearly, each λ corresponds to a zero of the Poincare-Melnikov Abelian integral $I(h)$. Therefore, the detection curve $\lambda(h)$ on the (h, λ) plane provides a visual tool in determining the number and locations of limit cycles. Since each family of closed orbits corresponds to one detection curve, we seek for all detection curves, representing all the families of the closed orbits, to intersect at the same $\lambda = \tilde{\lambda}$ line with the maximal number of intersections. Then the number and locations of limit cycles generated from each family of closed orbits through the perturbation are identified by the number and the location of intersections with respect to h. Note that the detection function $\lambda(h)$ is a ratio of two Abelian integrals over a family of closed orbits depending on the Hamiltonian level h. For the symmetric Hamiltonian system (1), within a symmetric closed orbit group and with the symmetric perturbation terms, the detection curves are identical. One detection curve can represent the whole group and the intersections, i.e., the number of limit cycles, can be expanded by multiply the number of members in the group, which makes the parameter control much simpler and efficient. But with sixth-degree perturbation terms in system (5), the divergence of the perturbation, i.e. the integration terms in the detection function integral are no longer symmetric with respect to the x-axis and the y-axis. Therefore, each detection curve must be considered separately even within the same group. Since the areas for the Abelian integrals bounded by the closed orbits are symmetric with both the x-axis and y-axis, it is desired to keep the symmetric advantages when choosing the control parameters. Preliminary numerical computation also indicates that it is more efficient to set parameters $s_{ij} = 0$ when $j = 1, 3, 5$, which makes the perturbation terms behave symmetrically with respect to the x-axis. Therefore, we only need to consider bifurcations of limit cycles on the x-axis and above. The number of limit cycles can be doubled for the closed orbits with mirror identities at the lower part of the plane.

It is obvious that the detection function $\lambda(h)$ is a ratio of two Abelian integrals over sixth-degree algebraic curves. Therefore, it can only be calculated numerically. The following are the formulae of $\phi(h)$ and $\psi_{ij}(h)$ for computing $J_{ij}(h)$ leading to the detection function λ:

$$\phi = \iint_{\Gamma_h} dx\,dy = \int (y_+ - y_-)\,dx, \quad \psi_{10} = \iint_{\Gamma_h} x\,dx\,dy = \int x(y_+ - y_-)\,dx,$$

$$\psi_{20} = \iint_{\Gamma_h} x^2 dx\,dy = \int x^2(y_+ - y_-)\,dx, \quad \psi_{02} = \iint_{\Gamma_h} y^2 dx\,dy = \frac{1}{3}\int (y_+^3 - y_-^3)\,dx,$$

$$\psi_{30} = \iint_{\Gamma_h} x^3 dx\,dy = \int x^3(y_+ - y_-)\,dx, \quad \psi_{12} = \iint_{\Gamma_h} xy^2 dx\,dy = \frac{1}{3}\int x(y_+^3 - y_-^3)\,dx,$$

$$\psi_{40} = \iint_{\Gamma_h} x^4 dx\,dy = \int x^4(y_+ - y_-)\,dx, \quad \psi_{22} = \iint_{\Gamma_h} x^2 y^2 dx\,dy = \frac{1}{3}\int x^2(y_+^3 - y_-^3)\,dx,$$

$$\psi_{04} = \iint_{\Gamma_h} y^4 dx\,dy = \frac{1}{5}\int (y_+^5 - y_-^5)\,dx, \quad \psi_{50} = \iint_{\Gamma_h} x^5 dx\,dy = \int x^5(y_+ - y_-)\,dx,$$

$$\psi_{32} = \iint_{\Gamma_h} x^3 y^2 dx\,dy = \frac{1}{3}\int x^3(y_+^3 - y_-^3)\,dx, \quad \psi_{14} = \iint_{\Gamma_h} xy^4 dx\,dy = \frac{1}{5}\int x(y_+^5 - y_-^5)\,dx.$$

With the aid of Maple [24], for a given value of h, the closed orbits corresponding to this value can be numerically obtained. For each family of closed orbits, the values of $\phi(h)$, $\psi_{ij}(h)$, and thus $J_{ij}(h)$ are calculated, which in turn gives the value of $\lambda(h)$ in terms of parameters. The parameter values of the first-order Hopf bifurcation at focus points on the upper half of the plane, $A_0, A_{2+},\ A_{2-},\ A_{4+}^U,\ A_{4-}^U,\ A_6^U,\ A_{8+}^U$ and A_{8-}^U, can be calculated based on the detection function theory [14,20]:

$$b_H = \lambda(h_i) + \mathrm{O}(\epsilon) = \lim_{h \to h_i} \lambda(h) + \mathrm{O}(\epsilon) = S(\xi, \eta) + \mathrm{O}(\epsilon), \tag{9}$$

where S is defined in (8), b_H is the first-order Hopf bifurcation parameter value at the focus point (ξ, η) and h is the Hamiltonian level at this focus point.

For each family of closed orbits, there exists one detection function curve $\lambda = \lambda(h)$ indicating the potential existence of limit cycles and their locations. Control conditions can be set by laying out all detection curves to make the maximal possible number of intersections at one line $\lambda = \tilde{\lambda}$. The solutions of the system of linear equations composed of control conditions are parameter desired to fulfil the objective. The results of bifurcations values calculated using Maple are displayed in Tables 3 and 4.

3. Computation of focus values for the existence of local limit cycles

In the previous section, we have discussed the computation of global bifurcations of limit cycles. Generally, for a limited number of perturbation parameters, there is limited flexibility in parameter control to satisfy both local and

Table 3
First-order Hopf bifurcations

h	Focus	Parameter values
h_0	A_0	$0 + O(\epsilon)$
h_2	A_{2-}	$2s_{20} - 2\sqrt{2}s_{30} + 4s_{40} - 4\sqrt{2}s_{50} - \sqrt{2}s_{10} + O(\epsilon)$
	A_{2+}	$2s_{20} + 2\sqrt{2}s_{30} + 4s_{40} + 4\sqrt{2}s_{50} + \sqrt{2}s_{10} + O(\epsilon)$
h_4	A_{4-}^U	$\frac{1}{2}s_{20} + 2s_{02} - \frac{1}{4}\sqrt{2}s_{30} + \frac{1}{4}s_{40} + 4s_{04} + s_{22} - \frac{1}{8}\sqrt{2}s_{50} - \frac{1}{2}\sqrt{2}s_{10} - \sqrt{2}s_{12} - 2\sqrt{2}s_{14} - \frac{1}{2}\sqrt{2}s_{32} + O(\epsilon)$
	A_{4+}^U	$\frac{1}{2}s_{20} + 2s_{02} + \frac{1}{4}\sqrt{2}s_{30} + \frac{1}{4}s_{40} + 4s_{04} + s_{22} + \frac{1}{8}\sqrt{2}s_{50} + \frac{1}{2}\sqrt{2}s_{10} + \sqrt{2}s_{12} + 2\sqrt{2}s_{14} + \frac{1}{2}\sqrt{2}s_{32} + O(\epsilon)$
h_6	A_6^U	$8s_{02} + 64s_{04} + O(\epsilon)$
h_8	A_{8-}^U	$2s_{20} + 8s_{02} - 2\sqrt{2}s_{30} + 4s_{40} + 64s_{04} + 16s_{22} - 4\sqrt{2}s_{50} - \sqrt{2}s_{10} - 8\sqrt{2}s_{12} - 64\sqrt{2}s_{14} - 16\sqrt{2}s_{32} + O(\epsilon)$
	A_{8+}^U	$2s_{20} + 8s_{02} + 2\sqrt{2}s_{30} + 4s_{40} + 64s_{04} + 16s_{22} + 4\sqrt{2}s_{50} + \sqrt{2}s10 + 8\sqrt{2}s_{12} + 64\sqrt{2}s_{14} + 16\sqrt{2}s_{32} + O(\epsilon)$

Table 4
Saddle-node bifurcations

h	λ	Parameter values
h_1	λ_0	$0.09660567545s_{20} + 0.05542969145s_{02} + 0.02033119566s_{40} + 0.006606314300s_{04} + 0.002852472700s_{22}$
	λ_1	$1.196811517s_{20} + 0.1223109725s_{02} + 2.190412406s_{40} + 0.3744837449s_{04} + 0.1949749145s_{22}$
	λ_{2-}	$1.706575249s_{20} + 0.1532994030s_{02} - 2.312410954s_{30} + 3.195886714s_{40} + 0.05173857653s_{04}$ $+ 0.2839919421s_{22} - 4.492011856s_{50} - 1.288933334s_{10} - 0.2073961794s_{12} - 0.07111888065s_{14} - 0.3931497212s_{32}$
	λ_{2+}	$1.706575249s_{20} + 0.1532994030s_{02} + 2.312410954s_{30} + 3.195886714s_{40} + 0.05173857653s_{04} + 0.2839919421s_{22}$ $+ 4.492011856s_{50} + 1.288933334s_{10} + 0.2073961794s_{12} + 0.07111888065s_{14} + 0.3931497212s_{32}$
h_3	λ_{4-}	$0.4414983175s_{20} + 1.973735690s_{02} - 0.3437887825s_{30} + 0.2829915226s_{40} + 4.184171632s_{04}$ $+ 0.8705814272s_{22} - 0.2422783810s_{50} - 0.6171961520s_{10} - 1.216974754s_{12} - 2.590537344s_{14} - 0.6782450839s_{32}$
	λ_{4+}	$0.4414983175s_{20} + 1.973735690s_{02} + 0.3437887825s_{30} + 0.2829915226s_{40} + 4.184171632s_{04} + 0.8705814272s_{22}$ $+ 0.2422783810s_{50} + 0.6171961520s_{10} + 1.216974754s_{12} + 2.590537344s_{14} + 0.6782450839s_{32}$
	λ_5^U	$0.4414983170s_{20} + 1.973735682s_{02} + 0.2829915227s_{40} + 4.184171627s_{04} + 0.8705814285s_{22}$
h_5	λ_1	$1.080881838s_{20} + 0.2992289455s_{02} + 1.928024472s_{40} + 0.2061954311s_{04} + 0.4105030244s_{22}$
	λ_5^U	$0.5298519663s_{20} + 1.911977133s_{02} + 0.5021482479s_{40} + 4.466898115s_{04} + 1.018713089s_{22}$
	λ_7^U	$1.101391930s_{20} + 6.753593284s_{02} + 2.099111549s_{40} + 50.27779340s_{04} + 7.344665471s_{22}$
	λ_O	$0.9425810912s_{20} + 3.727520403s_{02} + 1.624923236s_{40} + 24.58882463s_{04} + 3.792003542s_{22}$
h_7	λ_6^U	$0.09730649613s_{20} + 7.934940827s_{02} + 0.02054218059s_{40} + 63.24527129s_{04} + 0.7750411485s_{22}$
	λ_{7+}	$1.181206255s_{20} + 7.867506474s_{02} + 2.155850213s_{40} + 62.46922683s_{04} + 9.243207325s_{22}$
	λ_{8-}^U	$1.699351982s_{20} + 7.835270286s_{02} - 2.299930325s_{30} + 3.176609486s_{40} + 62.09824796s_{04}$ $+ 13.29131624s_{22} - 4.464038504s_{50} - 1.285770705s_{10} - 10.06401292s_{12} - 79.72497510s_{14} - 17.97992067s_{32}$
	λ_{8+}^U	$1.699351982s_{20} + 7.835270286s_{02} + 2.299930325s_{30} + 3.176609486s_{40} + 62.09824796s_{04}$ $+ 13.29131624s_{22} + 4.464038504s_{50} + 1.285770705s_{10} + 10.06401292s_{12} + 79.72497510s_{14} + 17.97992067s_{32}$

global bifurcation conditions. In this article, we consider a sixth-degree polynomial perturbation to a fifth-degree Z_2 symmetric Hamiltonian system. Taking into account the symmetric perturbation as mentioned in Section 2, there are still 11 non-zero parameters to be used. For the 13 focus points in the system under consideration, it is intended to include the second-order focus values, i.e., to study degenerate Hopf bifurcations.

First we briefly describe an efficient technique for computing local focus values, such that the local limit cycles around focus points can be investigated. There are a number of methods which can be used to compute focus values. One of them is the method of normal form associated with Hopf singularity [19]. Usually, normal form theory is employed before the application of center manifold theory in order to reduce the original equation to a lower dimensional system. A perturbation technique has been developed to unify the two methods and to compute the normal forms of Hopf and degenerate Hopf bifurcations directly for general n-dimensional systems [19]. In the following, a brief description is given for the perturbation method.

Consider the following general n-dimensional differential equation:

$$\frac{d\mathbf{x}}{dt} = A\mathbf{x} + \mathbf{F}(\mathbf{x}), \quad \mathbf{x} \in R^n, \quad \mathbf{F} : R^n \to R^n, \tag{10}$$

where $A\mathbf{x}$ represents the linear part of the system, and the nonlinear function $\mathbf{F}$ is assumed to be analytic, satisfying $\mathbf{F}(0) = 0$, i.e., $\mathbf{x} = 0$ is an equilibrium of the system. Further, assume that the Jacobian of system (10) evaluated at $\mathbf{x} = 0$ contains a pair of purely imaginary eigenvalues $\pm i$. Thus the Jacobian of system (10) can be assumed in the Jordan canonical form:

$$J = \begin{bmatrix} 0 & 1 & 0 \\ -1 & 0 & 0 \\ 0 & 0 & B \end{bmatrix}, \quad A \in R^{(n-2)\times(n-2)}, \tag{11}$$

where B is a Hurwitz matrix, i.e. all of its eigenvalues have negative real parts.

The basic idea of the perturbation technique is based on multiple scales, treating the time scale with space scale consistently. To achieve this, introducing the new independent time variables $T_k = \epsilon^k t$, $k = 0, 1, 2, \ldots$ to obtain partial derivatives with respect to T_k as follows:

$$\frac{d}{dt} = \frac{dT_0}{dt}\frac{\partial}{\partial T_0} + \frac{dT_1}{dt}\frac{\partial}{\partial T_1} + \frac{dT_2}{dt}\frac{\partial}{\partial T_2} + \cdots = D_0 + \epsilon D_1 + \epsilon^2 D_2 + \cdots \tag{12}$$

where $D_k = \frac{\partial}{\partial T_k}$ denotes a differentiation operator. Further, suppose the solutions of system (10) in the neighborhood of $\mathbf{x} = 0$ are expanded in the series:

$$\mathbf{x}(t; \epsilon) = \epsilon \mathbf{x}_1(T_0, T_1, \ldots) + \epsilon^2 \mathbf{x}_2(T_0, T_1, \ldots) + \cdots \tag{13}$$

where the perturbation parameter, ϵ, is the same as that in multiple scales, implying that both the time and space scalings are uniformed.

Now substituting (12) and (13) into system (10), and solving the resulting ordered linear differential equations yields the normal form, given in polar coordinates (the detailed procedure can be found in [19]):

$$\frac{dr}{dt} = \frac{\partial r}{\partial T_0}\frac{dT_0}{dt} + \frac{\partial r}{\partial T_1}\frac{dT_1}{dt} + \frac{\partial r}{\partial T_2}\frac{dT_2}{dt} + \cdots = D_0 r + D_1 r + D_2 r + \cdots \tag{14}$$

$$\frac{d\theta}{dt} = 1 + \frac{\partial\theta}{\partial T_0}\frac{\partial T_0}{\partial t} + \frac{\partial\theta}{\partial T_1}\frac{\partial T_1}{\partial t} + \frac{\partial\theta}{\partial T_2}\frac{\partial T_2}{\partial t} + \cdots = 1 + D_0\theta + D_1\theta + D_2\theta + \cdots \tag{15}$$

where $D_i r$ and $D_i \theta$ are uniquely determined. It can be shown that [20] the derivatives $D_i r$ and $D_i \theta$ are functions of r only, and only $D_{2k} r$ and $D_{2k} \theta$ are non-zero, which can be expressed as $D_{2k}\rho = v_k \rho^{2k+1}$ and $D_{2k}\phi = t_k \rho^{2k}$, where both v_k and t_k are expressed in terms of the original system's coefficients. v_k is called the kth-order focus value of the Hopf-type singularity. Therefore, the final normal form of system (10) associated with generalized Hopf singularities, up to $(2k + 1)$th order term, is described by

$$\frac{dr}{dt} = r(v_0 + v_1 r^2 + v_2 r^4 + \cdots + v_k r^{2k}), \tag{16}$$

$$\frac{d\theta}{dt} = 1 + t_1 r^2 + t_2 r^4 + \cdots + t_k r^{2k}, \tag{17}$$

where v_0 is the linear perturbation of the system and equals zero at the focus point $\mathbf{x} = 0$. The basic idea of finding k small limit cycles around the origin is as follows: First, find the conditions such that $v_1 = v_2 = \cdots = v_{k-1} = 0$, but $v_k \neq 0$, and then properly perturb these focus values to show the existence of k limit cycles.

A sufficient condition for system (16) and (17) to have k limit cycles is given in the following theorem. The proof can be found in [5–7].

Theorem 1 [5–7]. *If the focus values v_i in Eq. (16) satisfy the following condition*:

$$v_i v_{i+1} < 0 \quad and \quad |v_i| \ll |v_{i+1}| \ll 1, \quad for \ i = 0, 1, 2, \ldots, k-1,$$

then the polynomial equation given by $\frac{dr}{dt} = 0$ in Eq. (16) has k positive real roots of r^2, and thus the system has k limit cycles.

There are 13 Hopf-type focus points in system (5). Due to the symmetry, we consider 8 focus points on the x-axis and the upper half of the plane, symbolled as $A_0, A_{2+}, A_{2-}, A_{4+}^U, A_{4-}^U, A_6^U, A_{8+}^U$ and A_{8-}^U, see Fig. 1 and Table 1 for their detailed locations.

To analyze the local Hopf bifurcation at each point using the method of normal form described above, first introduce a transformation into system (5) to make the focus point at the origin. For example, substituting $x \rightarrow x + \sqrt{2}$, $y \rightarrow y + 2\sqrt{2}$ into the system can move the focus point A_{8+}^U to the origin of the transformed system. Then the Maple program developed in [19] is applied to obtain its focus values v_i. Here we consider up to second-order Hopf bifurcation associated with the focus value v_1. To be consistent with the previous global limit cycle investigation, which has taken care of perturbation order up to $O(\epsilon)$, we take into account the first approximation of v_1 by ignoring the $O(\epsilon^2)$ terms. For each of the 8 focus points, the first- and second-order focus values are calculated and listed in Table 2. Note that the first-order focus values are consistent with the first-order Hopf bifurcation values calculated by using the detection function method. According to Theorem 1, in general, when $v_0 = v_1 = 0$ at a focus point, one can perturb these two focus values to obtain two limit cycles. However, since $O(\epsilon^2)$ terms are ignored in calculating $v_1 = 0$, it is possible that the final values may yield one limit cycle or three limit cycles. Therefore, when all the parameter values are determined, one must recalculate the focus values up to higher order terms to check if the focus point indeed has two limit cycles. The procedure will be seen in the next section.

4. Parameter control of both local and global bifurcations of limit cycles

Thus far, we have considered global bifurcations of limit cycles that occur at homoclinic, heteroclinic and other periodic orbits, and local bifurcations of limit cycles that occur at focus points. Parameter values corresponding to each closed orbit around each critical point have been calculated. Now we are ready to set up control conditions to find parameter groups which can make the sixth-degree polynomial system (5) generate the maximal possible number of limit cycles. We have obtained two different parameter groups which produce, respectively, 31 and 35 limit cycles with different distributions.

4.1. Group one of parameter control

In this control group, suppose the following global bifurcation conditions hold:

$$\lambda_7^U(h_5) - \lambda_5^U(h_5) = 0, \quad \lambda_7^U(h_5) - \lambda_7^U(0) = 0,$$
$$\lambda_5^U(h_5) - \lambda_{4+}^U(h_3) = 0, \quad \lambda_5^U(h_5) - \lambda_1(h_1 + 0.15) = 0,$$
$$\lambda_{8+}^U(h_7) - \lambda_7^U(h_5) = 0, \quad \lambda_{8+}^U(h_7) - \lambda_{8+}^U(h_6) = 0, \tag{18}$$
$$\lambda_5^U(h_5) - \lambda_{4-}^U(h_4) - 0.00004 = 0, \quad \lambda_5^U(h_5) - \lambda_{4-}^U(h_3 + 0.05) = 0,$$
$$\lambda_5^U(h_5) - \lambda_{4+}^U(h_3 + 0.05) = 0.$$

The above 9 conditions can be expressed as a system of 9 linear equations with 11 unknowns, listed as follows:

$$C_1 : 0 = 0.5715399637 s_{20} + 4.841616151 s_{02} + 1.596963301 s_{40} + 45.81089528 s_{04} + 6.325952382 s_{22},$$

$$C_2 : 0 = 0.042718755 s_{20} - 0.564158365 s_{02} + 0.143809789 s_{40} - 6.00969047 s_{04} - 0.360632607 s_{22},$$

$$C_3 : 0 = 0.5439002537 s_{20} - 1.658783324 s_{02} + 1.405460563 s_{40} - 4.323022987 s_{04} - 0.6760110445 s_{22},$$

$$C_4 : 0 = 0.0883536488 s_{20} - 0.061758557 s_{02} + 0.3437887824 s_{30} + 0.2191567253 s_{40} + 0.282726483 s_{04}$$
$$+ 0.1481316618 s_{22} + 0.2422783813 s_{50} + 0.6171961524 s_{10} + 1.216974754 s_{12} + 2.590537344 s_{14}$$
$$+ 0.6782450837 s_{32},$$

$$C_5 : 0 = 0.597960045s_{20} + 1.081676956s_{02} + 2.299930318s_{30} + 1.077497930s_{40} + 11.82045417s_{04}$$
$$+ 5.946650419s_{22} + 4.464038485s_{50} + 1.285770703s_{10} + 10.06401275s_{12} + 79.72497468s_{14}$$
$$+ 17.97992044s_{32},$$

$$C_6 : 0 = -0.176477825s_{20} - 0.062136204s_{02} - 0.304472974s_{30} - 0.470252323s_{40} - 0.71345001s_{04}$$
$$- 1.51812430s_{22} - 0.683739099s_{50} - 0.077452985s_{10} - 0.69994775s_{12} - 5.87863771s_{14}$$
$$- 2.57960391s_{32},$$

$$C_7 : 0 = 0.0298519663s_{20} - 0.088022867s_{02} + 0.3535533904s_{30} + 0.2521482479s_{40} + 0.466898115s_{04}$$
$$+ 0.018713089s_{22} + 0.1767766955s_{50} + 0.7071067814s_{10} + 1.414213562s_{12} + 2.828427124s_{14} \qquad (19)$$
$$+ 0.7071067808s_{32},$$

$$C_8 : 0 = 0.0491163201s_{20} - 0.073113074s_{02} + 0.3580572593s_{30} + 0.2255258024s_{40} + 0.355874971s_{04}$$
$$+ 0.0645225853s_{22} + 0.2201301254s_{50} + 0.6750140723s_{10} + 1.339780091s_{12} + 2.776321103s_{14}$$
$$+ 0.7107887035s_{32} - 0.00004,$$

$$C_9 : 0 = 0.0491163233s_{20} - 0.073113071s_{02} - 0.3580572581s_{30} + 0.2255258046s_{40} + 0.355874993s_{04}$$
$$+ 0.0645225903s_{22} - 0.2201301240s_{50} - 0.6750140699s_{10} - 1.339780091s_{12} - 2.776321096s_{14}$$
$$- 0.7107887016s_{32}.$$

Note that in the above calculations with the aid of Maple, we have used the accuracy up to 30 decimal places. Here, we only present up to 10 decimal places for simplicity. Next, we want to solve system (19) to find the parameters values. For the 9 equations with 11 unknowns, there are two free variables to be determined. To avoid ill-condition in the resulting system, the two free variables are carefully chosen as s_{10} and s_{30}. Then the solution of system (19) is obtained as

$$s_{02} = 0.03276575104s_{30} + 0.08181904880s_{10} + 0.0003836612616,$$
$$s_{04} = -0.001246972416s_{30} - 0.003113803448s_{10} - 0.00001460107497,$$
$$s_{12} = -0.2536959004s_{30} - 0.6342296417s_{10} - 0.00003706042662,$$
$$s_{14} = 0.02361479041s_{30} + 0.05904288287s_{10} - 0.00001692066454,$$
$$s_{20} = 0.03199934567s_{30} + 0.07990527947s_{10} + 0.0003746871675, \qquad (20)$$
$$s_{22} = -0.2194212068s_{30} - 0.5479146047s_{10} - 0.0002569249953,$$
$$s_{32} = 0.04100838531s_{30} + 0.1024777764s_{10} + 0.0001889283679,$$
$$s_{40} = 0.01189860701s_{30} + 0.02971189456s_{10} + 0.0001393233970,$$
$$s_{50} = -0.5127470861s_{30} - 0.2818690593 - 0.0001710721296s_{10}.$$

The two free variables, s_{10} and s_{30}, are used to set conditions in examining degenerate Hopf bifurcations. Consider the focus point A_{4-}^U and substitute Eq. (20) into the formulas given in Table 2 to obtain

$$v_0 = \epsilon(0.001342173842 + 0.2879361036s_{10} + 0.1153086132s_{30} - 2\lambda),$$
$$v_1 = -10^{-15}(0.1334498023 \times 10^{-5}s_{30}^2 + 0.1745895734s_{30} + 7.2142551742),$$

where λ is the detection function defined in (7). Note that in the second equation λ and ϵ have been set as

$$\lambda = 0.005 \quad \text{and} \quad \epsilon = 10^{-10}$$

for simplicity. Then solving equation $v_0 = 0$ for s_{10} yields $s_{10} = -0.4004659777s_{30} + 0.03006856747$. In order to investigate the possibility of the existence of the second limit cycles around the focus point A_{4-}^U, let $v_1 = 0$. Solve $v_1 = 0$ for s_{30} to get two solutions: -130786.5654019026 and -41.3342850370. We take the second value and then s_{10} is also obtained:

$$s_{30} = -41.3342850370 \quad \text{and} \quad s_{10} = 16.5830434356.$$

Then from Eq. (20) we can determine all the parameter values, which may be called critical values. Under these critical values, we apply the Maple program [19] to find $v_2 = 0.1667990443 \times 10^{-12} > 0$. Now we want perturb these critical values such that the global structure are not changed (so the number of global limit cycles are remained the same), but

hope get two small limit cycles around the focus point A_{4-}^U. To achieve this, we use $\epsilon = 10^{-10}$ for the global perturbation (i.e., the perturbation on the whole Hamiltonian system) which will not affect the global structure of the system. For the local perturbations we perturb the coefficients s_{30} and s_{10}. In particular, we perturb v_1 using s_{30} such that $v_1 < 0$ and $-v_1 \ll v_2$. For example, suppose we want $v_1 \approx -10^{-17}$ after perturbation, then we may perturb s_{30} to $s_{30} + 0.01 = -41.3242850370$ under which $v_1 = -0.1744792658 \times 10^{-17}$, while then $s_{10} = -0.4004659777 s_{30} + 0.03006856747 = 16.5790387759$ for which v_0 is still equal to zero. Similarly, we perturb v_0 such that $v_0 > 0$ and $v_0 \ll -v_1$. For example, we may set $v_0 \approx 10^{-23}$, and thus we perturb s_{10} to $s_{10} + 10^{-13} = 16.5790387758598367486750935870$ under which $v_0 = 0.28793610361930005690562 \times 10^{-23}$. Now for the perturbed values s_{30} and s_{10}, we have

$$v_2 = 0.166784592983115626311 \times 10^{-12},$$

$$v_1 = -0.174479269148814169404 9 \times 10^{-17},$$

$$v_0 = 0.28793610361930005690562 \times 10^{-23}.$$

Therefore, the normal form associated with the focus point A_{4-}^U, given in Eq. (16) for $k = 2$, can be written as

$$\frac{\mathrm{d}r}{\mathrm{d}t} = 10^{-12}(0.28793610361930005690562 \times 10^{-11} - 0.1744792691488141694049 \times 10^{-5}r^2$$
$$+ 0.166784592983115626311 r^4),$$

which, in turn by setting $\frac{\mathrm{d}r}{\mathrm{d}t} = 0$, yields two positive roots:

$$r = 0.0028996728056034268787, \quad 0.0014329172186917924944, \tag{21}$$

indicating that there exist two limit cycles in the vicinity of the focus point A_{4-}^U. However, as pointed out early, due to ignoring the higher-order terms in determining the critical values (except for s_{30}, all other parameters are solved from linear equations which are ϵ-order terms), we need to check if higher-order focus values affect the results. Thus, for the following perturbed parameter values:

$$s_{02} = 0.0028437687689149195179046947 4000,$$

$$s_{04} = -0.000108231841334091253180834195549,$$

$$s_{10} = 16.5790387758598367486750935870,$$

$$s_{20} = 0.0027775162786007532289009224524 6,$$

$$s_{30} = -41.3242850370282949308745319183,$$

$$s_{40} = 0.00103259532312892335706150201947, \tag{22}$$

$$s_{50} = 16.5156175655002872992657204374,$$

$$s_{12} = -0.031153199263688617803 5328422852,$$

$$s_{14} = 0.0029929878725676224986132 2259400,$$

$$s_{22} = -0.0019043294676538457043 6243401314,$$

$$s_{32} = 0.0045298210880585012613965 8217068.$$

We execute the Maple program [20] to obtain the normal form up to $k = 6$:

$$\frac{\mathrm{d}r}{\mathrm{d}t} = 10^{-8}(0.28793610361929833557 \times 10^{-15} - 0.17447926914870000000 \times 10^{-9}r^2$$
$$+ 0.16678459298311562476 \times 10^{-4}r^4 - 0.02366759946415607382 r^6 - 0.04699003379514715609 r^8$$
$$- 0.13047272993815828422 r^{10} - 0.38785791320809525520 r^{12}).$$

Solving the equations $\frac{\mathrm{d}r}{\mathrm{d}t} = 0$ yields the solutions:

$$r^2 = 0.20513248238306781857 \times 10^{-5}, \quad 0.85444776034661038713 \times 10^{-5}, \quad 0.69312956681688582588 \times 10^{-3},$$
$$- 0.40735337730851201421, \quad 0.03512827061386311063 \pm 0.38571383330043643328 i,$$

which clearly shows that there are three positive solutions. Hence, there actually exist three limit cycles around A_{4-}^U with the amplitudes, given by

$$r = 0.00143224468015443443, \quad 0.00292309384102975796, \quad 0.02632735396535105322. \quad (23)$$

Comparing Eq. (23) with Eq. (21) shows that the first two roots given in Eq. (23) are almost identical to that given in Eq. (21). The third root given in Eq. (23) comes from $v_3 = -0.38309145060960631437 \times 10^{-9}$ which happens to have opposite sign of v_2 and satisfy $|v_2| \ll |v_3|$, though we did not calculate the general symbolic form of v_3 since its expression is too long to handle in symbolic computation. In fact, even the general expression of v_2 has already had over 800 lines in printing. However, this is not always the case, that is, one cannot always expect to have one more limit cycle than that assumed in calculation. In fact, sometimes the expected number of limit cycles may be reduced. This will be seen in the next subsection when we consider group two of parameter control.

Having found three small limit cycles around the focus point A_{4-}^U, we count its mirror point at the lower part of the plane to have a total of 6 local small limit cycles for the system. The values for this set of parameters are shown in Eq. (22), which lead to the detection function graphs shown in Fig. 3(a) and its zoom-in in Fig. 3(b). These graphs show that the straight line $\lambda = 0.005$ intersects with λ_{4+}^U and λ_7^U three points each, with λ_{4-}^U, λ_{8+}^U, λ_5^U and λ_1 two points each, and with λ_O at one point. Each intersection indicates one limit cycle. Due to symmetry, points A_{4+}^U, A_{4-}^U, A_5^U, A_7^U and A_{8+}^U all have identical mirrors on the lower part of the plane. Therefore, any limit cycles corresponding to these fixed points shall be doubled, which makes the total of 27 limit cycles including the first-order Hopf bifurcation at the point A_{4-}^U. Therefore 4 higher-order local limit cycles at the focus point A_{4-}^U should be added into the total number, resulting in the total of 31 limit cycles for this group of parameters. The configuration of this set of limit cycles is shown in Fig. 4.
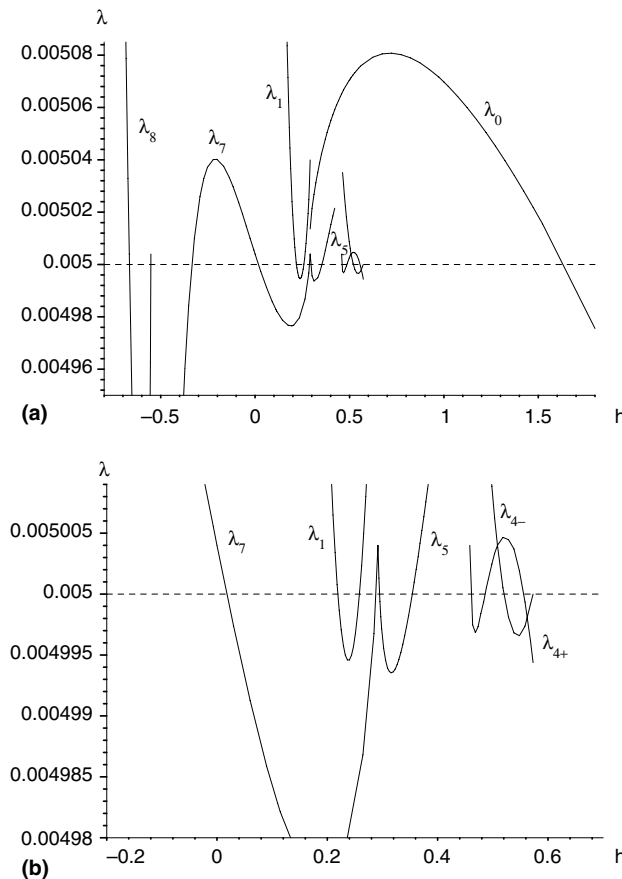

Fig. 3. The detection curves for parameter group one: (a) the graph of the detection curves for Eq. (5); and (b) a zoom-in of part (a).
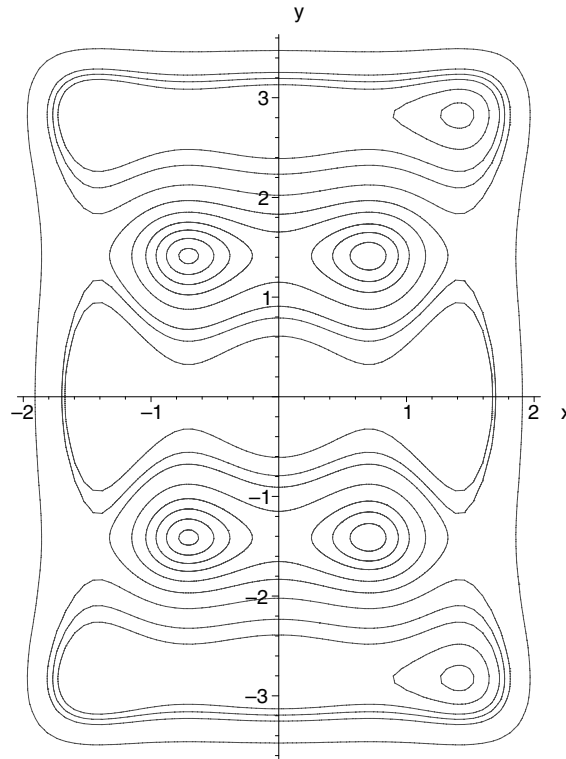
Fig. 4. The layout of the 31 limit cycles for parameter group one.

4.2. Group two of parameter control

Now we turn to another control group, which satisfies the following global conditions:

$$
\begin{aligned}
&\lambda_7^U(h_5) - \lambda_7^U(0) = 0, \quad \lambda_7^U(h_5) - \lambda_5^U(h_5) = 0, \\
&\lambda_{8+}^U(h_7) - \lambda_7^U(h_5) = 0, \quad \lambda_{8+}^U(h_8) - \lambda_{8+}^U(h_6) = 0, \\
&\lambda_{8+}^U(h_7) - \lambda_{4-}^U(h_3) = 0, \quad \lambda_{4-}^U(h_4) - \lambda_{4-}^U(h_3 + 0.045) = 0.
\end{aligned}
\tag{24}
$$

This condition group considers Hopf bifurcations at the three focus points: A_{8+}^U, A_{4-}^U and A_{4+}^U. We add the second-order Hopf bifurcation conditions at these focus points, which makes the condition group become a system of 6 linear equations with 11 unknowns, listed as follows:

$$
\begin{aligned}
C_1 : 0 =\ & 0.042718755 s_{20} - 0.564158365 s_{02} + 0.143809789 s_{40} - 6.00969047 s_{04} - 0.360632607 s_{22}, \\
C_2 : 0 =\ & 0.5715399637 s_{20} + 4.841616151 s_{02} + 1.596963301 s_{40} + 45.81089528 s_{04} + 6.325952382 s_{22}, \\
C_3 : 0 =\ & 0.597960045 s_{20} + 1.081676956 s_{02} + 2.299930318 s_{30} + 1.077497930 s_{40} \\
& + 11.82045417 s_{04} + 5.946650419 s_{22} + 4.464038485 s_{50} + 1.285770703 s_{10} \\
& + 10.06401275 s_{12} + 79.72497468 s_{14} + 17.97992044 s_{32}, \\
C_4 : 0 =\ & -0.124170200 s_{20} - 0.102593556 s_{02} - 0.224023832 s_{30} - 0.353138198 s_{40} \\
& - 1.18830242 s_{04} - 1.19055981 s_{22} - 0.509076665 s_{50} - 0.050989874 s_{10} \\
& - 0.54974800 s_{12} - 4.90605558 s_{14} - 2.06789264 s_{32}, \\
C_5 : 0 =\ & 1.257853658 s_{20} + 5.861534550 s_{02} + 2.643719100 s_{30} + 2.893617956 s_{40} \\
& + 57.91407594 s_{04} + 12.42073446 s_{22} + 4.706316865 s_{50} + 1.902966855 s_{10} \\
& + 11.28098750 s_{12} + 82.31551202 s_{14} + 18.65816552 s_{32}, \\
C_6 : 0 =\ & 0.0214024448 s_{20} + 0.016100490 s_{02} + 0.0044154173 s_{30} - 0.0283600445 s_{40} \\
& - 0.119189670 s_{04} + 0.0506485502 s_{22} + 0.0464926702 s_{50} - 0.0354529874 s_{10} \\
& - 0.081942393 s_{12} - 0.060169666 es_{14} + 0.0030779389 s_{32}.
\end{aligned}
\tag{25}
$$

The solutions of system (25) have 5 free variables to be determined. To avoid ill-conditioned coefficient matrix for solving the linear system, the five free variables are carefully selected as s_{10}, s_{12}, s_{14}, s_{30} and s_{32}. Then the solutions of system (25) given in terms of these five free variables are:

$$
\begin{aligned}
s_{02} &= 0.9720580740 s_{30} + 2.430252778 s_{10} - 1.957515146 s_{12} - 52.99733402 s_{14} - 2.825634586 s_{32}, \\
s_{04} &= -0.1211725002 s_{30} - 0.3029393098 s_{10} - 0.04482923874 s_{12} + 3.962209968 s_{14} + 0.2549532493 s_{32}, \\
s_{20} &= -1.201464605 s_{30} - 3.003786292 s_{10} + 3.356252990 s_{12} + 70.00066905 s_{14} + 9.700530669 s_{32}, \\
s_{22} &= 0.2863522411 s_{30} + 0.7158539050 s_{10} + 2.561332324 s_{12} + 13.15267104 s_{14} + 0.1690147122 s_{32}, \\
s_{40} &= -0.1753809613 s_{30} - 0.4383969924 s_{10} - 4.126515946 s_{12} - 30.13906964 s_{14} - 2.888243285 s_{32}, \\
s_{50} &= -0.6080828790 s_{30} - 0.5201693031 s_{10} - 4.526988862 s_{12} - 35.13214692 s_{14} - 4.845541744 s_{32}.
\end{aligned}
\tag{26}
$$

The five free variables are used in examining higher order Hopf bifurcations at the three focus points A_{4-}^{U}, A_{4+}^{U} and A_{8+}^{U}. Similar to the case considered in the group one of parameter control, we try to use the five free variables to set the first- and second-order focus values zero at the three focus points. The focus values are listed in Table 2. Since there are only five free parameters, we cannot let all the three v_0s and three v_1s zero. We choose to set $v_0 = v_1 = 0$ for A_{8+}^{U} and A_{4-}^{U}, but only $v_0 = 0$ for A_{4+}^{U}. The order of solving the five equations is: $v_0^{8+} = v_1^{8+} = v_0^{4+} = v_0^{4-} = v_1^{4-} = 0$, where the superscripts denote the focus points. The parameter order for solving the five equations is: s_{30}, s_{14}, s_{12}, s_{32} and s_{10}. The solutions are given below:

$$
\begin{aligned}
s_{30} &= 0.11271437276864112863 + 54.93383508871581048574 s_{14} \\
&\quad - 2.50011747863523396886 s_{10} + 0.58482030553969977819 s_{32} + 1.84427851842337848796 s_{12}, \\
s_{14} &= -0.00022269497908706250 + 0.00002255253349379309 s_{10} \\
&\quad - 0.14177789711811484132 s_{32} - 0.07966540620370250299 s_{12}, \\
s_{12} &= -0.0887722783743796896 - 0.00081329426541121150 s_{10} + 5.05927467199378308832 s_{32}, \\
s_{32} &= 0.01887104726437523464 - 0.00004299435194368912 s_{10}, \\
s_{10} &= \{ x | f(x) \equiv 0.82995570399407325442 \times 10^{-6} x^2 + 0.39405332783814565648 x \\
&\quad + 12.31108786335826291733 = 0 \},
\end{aligned}
\tag{27}
$$

where λ and ϵ have been set as $\lambda = 0.1$ and $\epsilon = 10^{-10}$. Note that the first four equations in (27) are obtained from the ϵ terms (leading to linear equations), while the last equation in (27) includes ϵ^2 terms, resulting a quadratic equation. From the last equation of (27) we can find a solution $s_{10} = -31.24424335137135221334$. (The another very large solution is not chosen.) Then all the other critical parameter values are obtained, which are substituted into the focus values to obtain

$$
\begin{aligned}
v_0^{8+} &= 0.181 \times 10^{-36}, \\
v_1^{8+} &= 0.40375804981566355762 \times 10^{-16}, \\
v_2^{8+} &= -0.96983280107200255059 \times 10^{-12}, \\
v_0^{4+} &= -0.10403779771774277801^{-37}, \\
v_1^{4+} &= -0.45417942563917687127 \times 10^{-13}, \\
v_2^{4+} &= 0.35644976693833768354 \times 10^{-12}, \\
v_0^{4-} &= -0.25571220228225722199 \times 10^{-37}, \\
v_1^{4-} &= -0.14 \times 10^{-37}, \\
v_2^{4-} &= -0.28346460714959506301 \times 10^{-12},
\end{aligned}
$$

which shows that $v_0^{8+} = v_0^{4+} = v_0^{4-} = v_1^{4-} = 0$. Thus, in the neighborhood of A_{4-}^{U}, at least two small limit cycles can be obtained after appropriate perturbations. For A_{4+}^{U}, at least one small limit cycle exists. Note that although $v_1^{4+} v_2^{4+} < 0$, their order difference is not large enough, so most likely one cannot get a second limit cycle. For A_{8+}^{U}, note that $v_1^{8+} \neq 0$. But since $v_1^{8+} v_2^{8+} < 0$ and $|v_1^{8+}| \ll |v_2^{8+}|$, one can still have two limit cycles around A_{8+}^{U} even without perturbing s_{14}. Therefore, at least 5 small limit cycles can be obtained from the three focus points.

A careful examination provides a suitable set of perturbations, given below:

$$
s_{10} \to s_{10} - 10^{-3}, \quad s_{32} \to s_{32} - 10^{-13}, \quad s_{12} \to s_{12} + 10^{-12}, \quad s_{30} \to s_{30} - 10^{-14},
$$

under which the perturbed parameters are:

$$s_{02} = 0.054966235904646218053992889089 0,$$
$$s_{04} = -0.001997279849872524401079561652 50,$$
$$s_{10} = -31.245243351371352213338002831 1,$$
$$s_{20} = 0.062752759445353064750424737700 0,$$
$$s_{30} = 77.934425645154496678204144421 5,$$
$$s_{40} = 0.018420023953930417515116180200 0,$$
$$s_{50} = -31.169689974497305508887846434 6,$$
$$s_{12} = 0.038904633563033105945372914716 0,$$
$$s_{14} = -0.068926652401858883914400941301 2,$$
$$s_{22} = -0.037924738120713972272907474435 8,$$
$$s_{32} = 0.202144162534903070756675579436.$$

(28)

With the above perturbed parameter values, in order to find the exact limit cycles which may exist in the vicinities of the three focus points, we again execute the Maple program [19] up to $k = 6$ to obtain the following normal forms:

$$\frac{\mathrm{d}r}{\mathrm{d}t} = 10^{-11}(-0.17743966016693497 \times 10^{-12} + 0.40378395967520000000 \times 10^{-5}r^2 - 0.09698580268064667584r^4$$
$$+ 0.06072444132305964342r^6 + 0.39575511657163542112r^8 + 0.83909717543052170954r^{10}$$
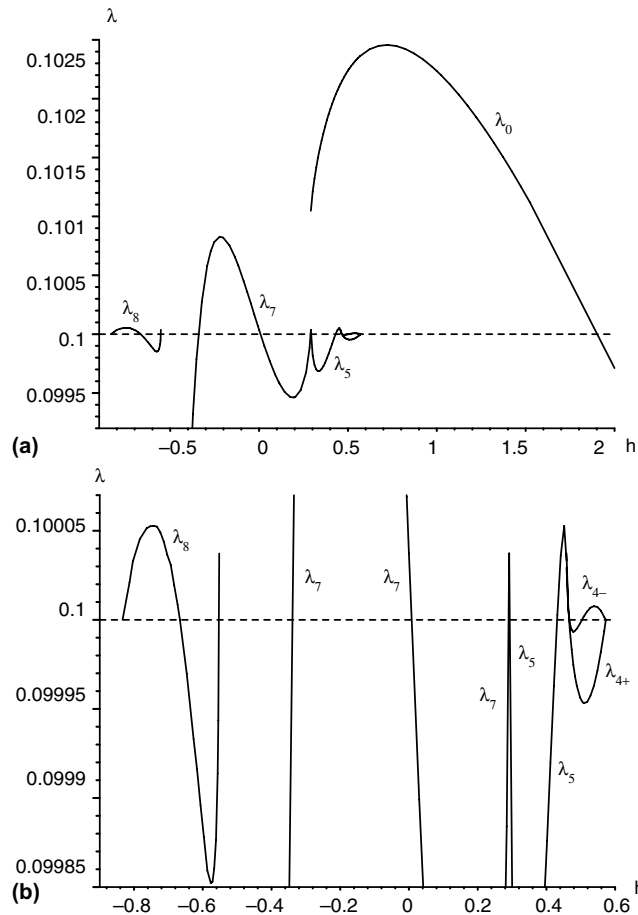$$+ 6.25344679173949611381r^{12}).$$

Fig. 5. The detection curves for parameter group one: (a) the graph of the detection curves for Eq. (5); and (b) a zoom-in of part (a).

for A_{8+}^U,

$$\frac{\mathrm{d}r}{\mathrm{d}t} = 10^{-9}(0.10362452178645170854 \times 10^{-12} - 0.45455922757037186000 \times 10^{-4}r^2$$
$$+ 0.35644730271889475150 \times 10^{-3}r^4 - 0.44648099476659283667r^6 - 0.88681565879094584288r^8$$
$$- 2.46227509706969767205r^{10} - 7.31874249126255014454r^{12}).$$

for A_{4+}^U, and

$$\frac{\mathrm{d}r}{\mathrm{d}t} = 10^{-9}(0.28793610361929833557 \times 10^{-15} + 0.39400149875790000000 \times 10^{-8}r^2$$
$$- 0.28350058882253264350 \times 10^{-3}r^4 + 0.44691846825234635597r^6 + 0.88726039867955753820r^8$$
$$+ 2.46343018305992805797r^{10} + 7.32350939052446478801r^{12}).$$

for A_{4-}^U. Solving the above three polynomial equations $\frac{\mathrm{d}r}{\mathrm{d}t} = 0$ yields the following positive solutions for the amplitudes of the limit cycles. Three limit cycles for A_{8+}^U:

$$r = 0.00020973957381101313, \quad 0.00644906192745871977, \quad 0.52159534973890180822;$$

one limit cycle for A_{4+}^U:

$$r = 0.00004774589453081618;$$

and three limit cycles for A_{4-}^U:

$$r = 0.00113736088342050406, \quad 0.00359099188439600840, \quad 0.02488725842926630350.$$

Due to the symmetry, there are a total of 14 small limit cycles for this group of parameters. Given the parameter values in Eq. (28), the global limit cycles are obtained, as shown in Fig. 5(a) along with its zoom-in depicted in Fig. 5(b). These two figures clearly show how the detection curves intersect with single straight line $\lambda = 0.1$. There are three intersections on each of the curves corresponding to the points A_{4-}^U, A_{8+}^U and A_7^U; and two intersections on the curves
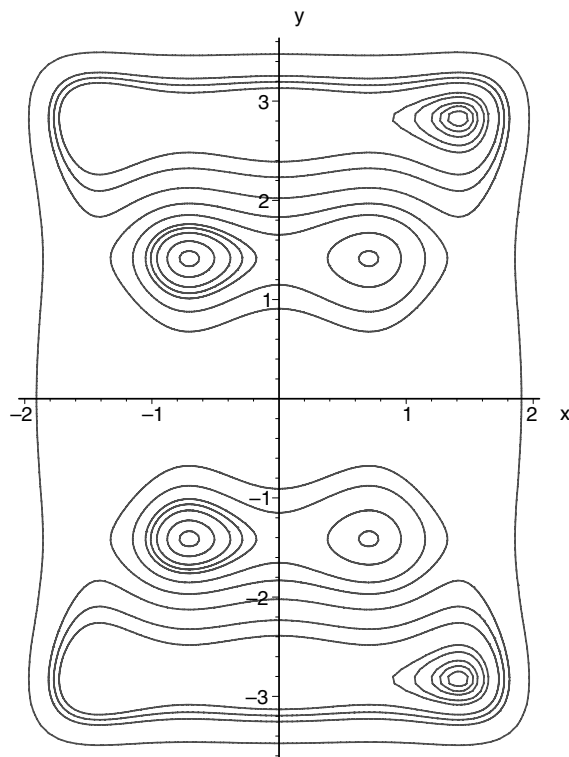

Fig. 6. The layout of the 35 limit cycles for parameter group two.

corresponding to the points A_5^U and A_{4+}^U; and one on the curve corresponding to the very outside annulus. Therefore, there are 27 global limit cycles generated under this group of parameters, which include the first-order Hopf limit cycles. Without counting redundantly, we shall add 8 higher-order Hopf limit cycles to the 27 global ones, which makes a total of 35 limit cycles for this perturbed system (5). Fig. 6 depicts the distribution of the 35 limit cycles.

Summarizing the results obtained in this section gives the main theorem of this paper as follows.

Theorem 2. *For the* 6*th-degree perturbed Hamiltonian vector field* (3) *with the control parameter group given in Eq.* (24), *and the perturbed parameter group listed in Eq.* (28) *when* $\lambda = 0.1$ *and* $\epsilon = 10^{-10}$, *the system has at least* 35 *limit cycles, i.e.,* $H(6) \geqslant 35 = 6^2 - 1$.

5. Conclusion

We take detour to study bifurcation of limit cycles for sixth-degree polynomial planar systems. We utilize the advantage of symmetric fifth-degree polynomial Hamiltonian system by adding a sixth-degree perturbation. The detection function method is applied for global bifurcation computation while the method of normal forms is used for local Hopf bifurcation calculation. The general sixth-degree perturbation of 20 terms is considered, followed by 11 dominant perturbation terms which are symmetric with respect to the x-axis in Abelian integrals. Numerical computation gives rise to the maximal of 35 limit cycles generated from the sixth-degree system. It matches the previous conjecture for odd degree systems [14,15] as $H(n) \geqslant n^2 - 1$ or $H(n) \geqslant n^2$. Further study is expected for the bifurcation of limit cycles in higher even degree systems.

References

[1] Ilyashenko Y. Centennial history of Hilbert's 16th problem. Am Math Soc 2002;39:301–54.
[2] Smale S. Mathematical problems for the next century. Math Intell 1998;20:7–15.
[3] Arnold VI. Loss of stability of self-oscillations close to resonance and versal deformations of equivariant vector fields. Funct Anal Appl 1977;11:85–92.
[4] Guckenhelmer J, Rand R, Schlomiuk D. Degenerate homoclinic cycles in perturbations of quadratic Hamiltonian systems. Nonlinearity 1989;2:405–18.
[5] Yu P, Han M. Twelve limit cycles in a 3rd-order planar system with Z_2 symmetry. Commun Appl Pure Anal 2004;3:515–26.
[6] Yu P, Han M. Twelve limit cycles in a cubic case of the 16th Hilbert problem. Int J Bifurcation & Chaos 15(7), in press.
[7] Yu P, Han M. Small limit cycles bifurcating from fine focus points in cubic order Z_2-equivariant vector fields. Chaos, Solitons & Fractals 2005;24:329–48.
[8] Melnikov VK. On the stability of the center for time periodic perturbations. Trans Moscow Math Soc 1963;12:1–57.
[9] Ye Y. Qualitative theory of polynomial differential systems. In: Modern Mathematics Series. Shanghai: Scientific and Technical Publishers; 1995 (in Chinese).
[10] Zhang Z, Ding T, Huang W, Dong Z. Qualitative theory of differential equations. Trans Math Monographs, vol. 101. Providence: American Mathematical Society; 1992.
[11] Zhang T, Han M, Zang H, Meng X. Bifurcation of limit cycles for a cubic Hamiltonian system under quartic perturbations. Chaos, Solitons & Fractals 2004;22:1127–38.
[12] Li J, Chan H, Chung K. Bifurcations of limit cycles in a Z_6-equivariant planar vector field of degree 5. Sci China (Ser A) 2002;45:817–26.
[13] Li J, Zhang M. Bifurcations of limit cycles in a Z_8-equivariant planar vector field of degree 7. J Differen Equations Dyn Syst 2004;16:1123–39.
[14] Wang S, Yu P, Li JB. Bifurcation of limit cycles in a Z_{10}-equivariant vector fields of degree 9. Int J Bifurcation & Chaos (accepted for publication).
[15] Wang S, Yu P. Existence of 121 limit cycles in a perturbed planar polynomial Hamiltonian vector field of degree 11. Nonlinearity (submitted for publication).

[16] Schlomiuk D. On the global analysis of the planar quadratic vector fields. Nonlinear Anal, Theory, Methods & Appl 1997;30:1429–37.
[17] Llibre J, Schlomiuk D. The geometry of quadratic differential systems with a weak focus of third order. Can J Math 2004;56(2):310–43.
[18] Li J, Li C. Planar cubic Hamiltonian systems and distribution of limit cycles of (E_3). Acta Math Sin 1985;28:509–21.
[19] Yu P. Computation of normal forms via a perturbation technique. J Sound Vib 1998;211:19–38.
[20] Li J. Hilbert's 16th problem and bifurcations of planar polynomial vector fields. Int J Bifurcation & Chaos 2003;13:47–106.
[21] Chen G, Wu Y, Yang X. The number of limit cycles for a class of quintic Hamiltonian systems under Quintic perturbations. J Austral Math Soc 2002;73:37–53.
[22] Li J, Zhou H. On the control of parameters of distributions of limit cycles for a Z_2-equivariant perturbed planar hamiltonian polynomial vector field. Int J Bifurcation & Chaos 2005;15.
[23] Carr J, Chow SN, Hale JK. Abelian integrals and bifurcation theory. J Differen Equations 1985;59:413–7.
[24] Corless R. Essential Maple 7: an introduction for scientific programmers. New York: Springer-Verlag; 2002.